Test Results from a Digital P(Y) Code Beamsteering GPS Receiver Designed for Carrier-Phase Time Transfer

Alison Brown, Neil Gerein, *NAVSYS Corporation;* Ed Powers*, US Naval Observatory*

BIOGRAPHY

Alison Brown is the President and CEO of NAVSYS Corporation. She has a PhD in Mechanics, Aerospace, and Nuclear Engineering from UCLA, an MS in Aeronautics and Astronautics from MIT, and an MA in Engineering from Cambridge University. In 1986 she founded NAVSYS Corporation. Currently she is a member of the GPS-III Independent Review Team and Scientific Advisory Board for the USAF and serves on the GPS World editorial advisory board.

Neil Gerein is a Product Manager for NAVSYS Corporation's Receivers Group and is responsible for the management and development of NAVSYS' next generation of GPS receivers. He is currently completing his M.Sc. in Electrical Engineering and holds a BSEE in Electrical Engineering from the University of Saskatchewan.

Edward Powers is employed as an electronic engineer working in the Time Transfer section of the Untied States Naval Observatory (USNO) in Washington DC. Previously he worked with the Naval Research Laboratory (NRL) conducting research on various projects related to precise time keeping and GPS satellite clock development. He received both his BS and MS in Engineering from the University of Arkansas (84, 87).

ABSTRACT

The development of time transfer techniques using GPS carrier-phase observations promises the capability to deliver sub-nanosecond time transfer capabilities. NAVSYS' High-gain Advanced GPS Receiver (HAGR) has been designed to enhance the accuracy of the GPS observations by using digital beam-steering from an antenna array. This provides over 10 dB of additional signal gain on each satellite tracked which improves the accuracy of both the code and carrier tracking loops, simplifying integer ambiguity resolution for carrier phase time transfer. This same design provides a highly phase stable observation of the GPS carrier, relative to a local reference oscillator, that enables precise time observations to be made for carrier-phase time transfer.

In this paper, the design of NAVSYS' P(Y) L1/L2 Code HAGR, developed for precise time transfer applications, is described and test results are included showing the accuracy of the code and carrier phase observations.

INTRODUCTION

GPS carrier-phase measurements provide the potential for much improved precision in time and frequency transfer [123456]. Because carrier phase observations are 100 to 1000 times more accurate than code based pseudo-range measurements, time transfer errors approaching 100 picosecond (ps) are expected using this approach.

The key to reliable carrier phase time transfer is the ability to resolve the carrier cycle ambiguity between the carrier phase and the pseudo-range to the satellite and also to determine which carrier phase cycle a given receiver is tracking, related to an external reference clock in a calibrated fashion.

This is achieved in the P(Y) High-Gain Advanced GPS Receiver (HAGR) design through the following innovations that are described further in this paper.

1. **Digital beam-steering phased array**. The digital beam-steering provides gain in the direction of the GPS satellites, as shown in Figure 1. This increases the measurement precision, and reduces multipath errors improving the ability to perform cycle ambiguity resolution.

2. **Phase coherent Digital Front-End (DFE)**. The phase coherent DFE samples the received GPS signals with a clock precisely synchronized and calibrated in phase to an external reference. This allows

unambiguous phase observations to be made coherent with the external time reference to be synchronized.

3. **Phase coherent frequency synthesis**. The frequency synthesizer is designed to generate the receiver Local Oscillator (LOs) for downconversion synchronized to the external time reference both in frequency and also with an unambiguous phase offset. This removes any ambiguous phase offset at start-up from the synthesizer phase-locking to the external reference.

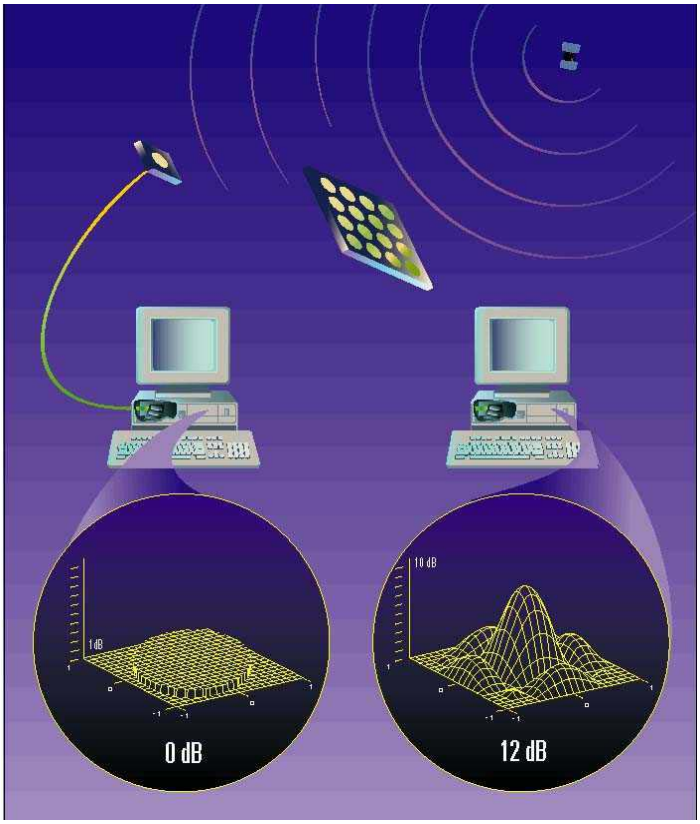

Figure 1 HAGR Digital Beamsteering Array

P(Y) HAGR DESIGN

The P(Y) HAGR is based on a modular, software and firmware reprogrammable digital GPS receiver design[7]. The system architecture, shown in Figure 2, uses an RF-to-Digital Front End (DFE) to digitize each of the antenna inputs from an array of antenna elements. Digital signal processing is then used to create an optimal beam pattern for each of the satellites tracked.

The receiver can be configured based on the user's requirements. In Figure 2 a P(Y) HAGR configuration is shown which is being delivered to the US Naval Observatory for a carrier time transfer application. This receiver is configured to provide the following capabilities.

- 16-element digital beam-steering on both the L1 and L2 frequencies
- 12 satellite tracking channels
- C/A (L1) and P(Y) (L1 and L2) observations
- Precise time synchronization (code and carrier phase) to an external time reference.

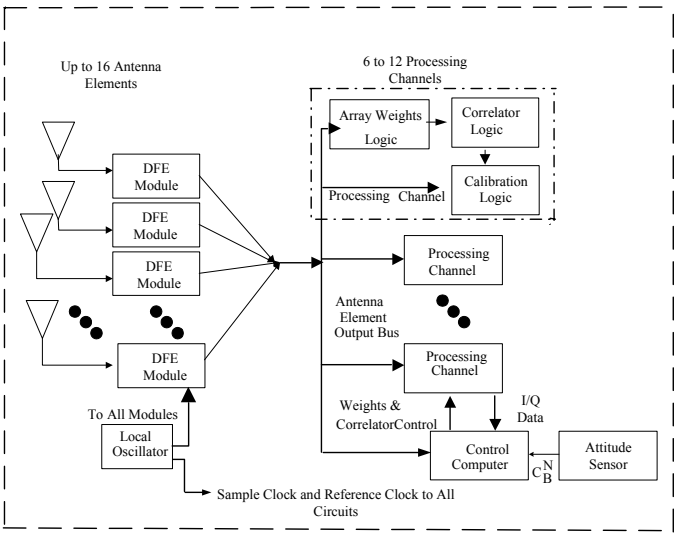

Figure 2 P(Y) HAGR System Architecture

The components of this receiver are shown in Figure 3 and are described further below.

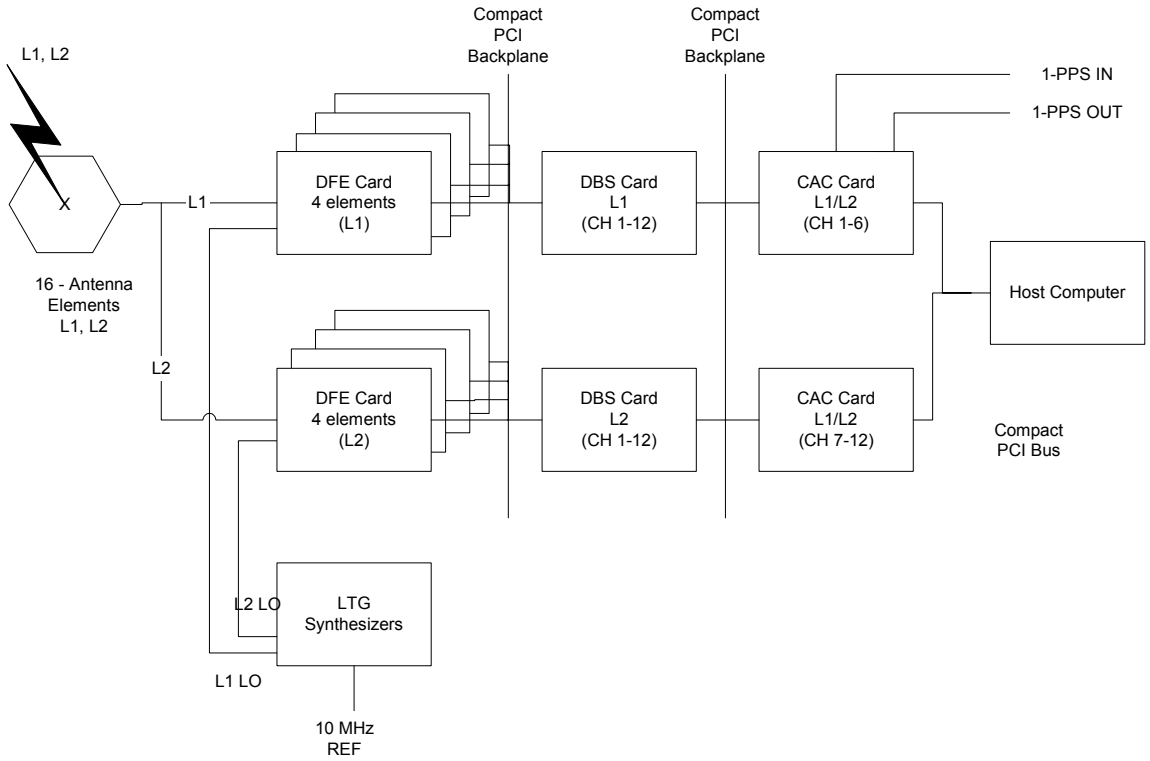

Figure 3 12-Channel P(Y) HAGR System Components

Antenna Array

The antenna array consists of 16 dual frequency elements laid out on a 4x4 antenna pattern. The elements are separated by 0.5 cycles at the L1 frequency. As described later, this provides optimal beam-steering performance at the L1 frequency, while some spatial aliasing occurs with the L2 frequency beam-forming.

Figure 4 L1/L2 16-element Antenna Array

Digital Front-End (DFE) Cards

The DFE cards perform the RF to digital conversion on each of the antenna inputs. Each card includes the capability to handle up to four antenna inputs. The frequency (L1 or L2) of each channel is selected by the front-end filter and by using either the L1 or L2 LO provided from the Local Time Generator (LTG) synthesizers. To handle 16 RF inputs at L1 and 16 RF inputs at L2, the P(Y) HAGR is configured with eight of the DFE cards shown in Figure 5.

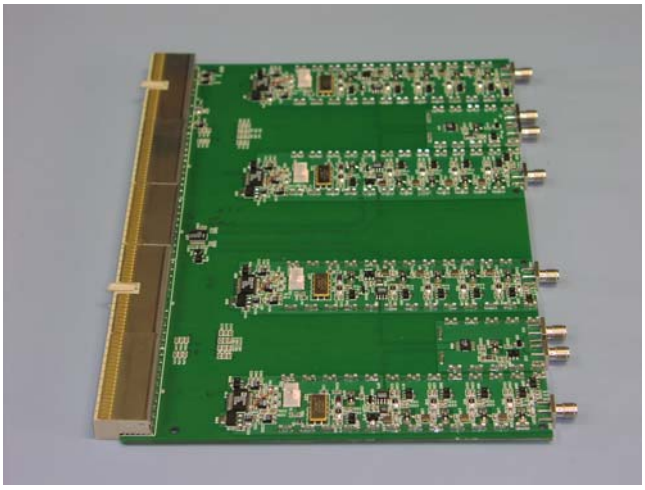

Figure 5 Digital Front End (DFE) Board

Digital Beam Steering (DBS) Card

The DBS card includes the digital logic to apply the beam-steering weights to the L1 and L2 digitized RF inputs. Each card can provide 12 digital beam-steering outputs from up to 16 digital antenna inputs from the DFE

cards. To provide beam-steering on 12 satellite channels, L1, and 12 satellite channels, L2, two DBS cards are included.

Correlation Accelerator Card (CAC) Card

The CAC performs the C/A and P(Y) code generation and correlation functions on the digital beam-steered signal outputs for each of the satellite channels. Each CAC card is configured to handle six satellite channels. Each channel provides the I/Q correlator outputs (Early, Prompt and Late) for the C/A (L1), P(Y) L1 and the P(Y) L2 signals. P(Y) code operation requires that the CAC card be keyed for PPS-SM operation through a KYK-13 interface. Two CAC cards are included to allow tracking on up to 12 satellites simultaneously.

Local Time Generator (LTG) Synthesizers

In an off-the-shelf RF phase-locked synthesizer design, the local oscillator signal F_0 is phase locked to the input reference clock by feeding back to the PLL phase comparator a divided version of the output F_0 signal. In commercial PLL synthesizer chips, this feedback division is free running, and as a result the synthesizer can lock to any number of N ambiguous initial phases (N is the feedback division ratio) as shown in Figure 6. Test results showing this effect from two L1 synthesizers is shown in Figure 7. Both synthesizers are locked to the same 10 MHz reference. One of the synthesizers is powered down and re-started periodically. The observed LO phase from turn-on to turn-on changes due to the different start times of the synthesizer divide chain.

To eliminate this phase ambiguity, NAVSYS have come up with a proprietary L1 and L2 synthesizer design that forces a known phase synchronization of the feedback divider chains of both L1 and L2 LO channels synchronous to an external event marker (typically a 1PPS strobe). This removes the potential for the ambiguous synthesizer phase offsets at start-up as shown in Figure 7.

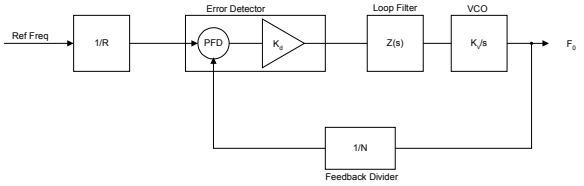

Figure 6 Synthesizer Frequency Locked Divide Chain

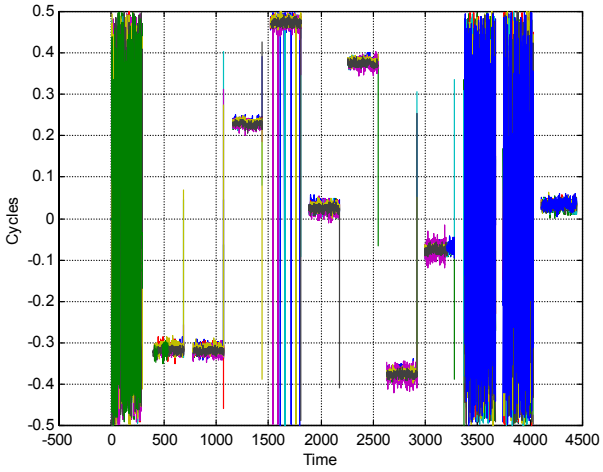

Figure 7 Conventional Synthesizer turn-on to turn-on phase offset

Host Computer

A COTS 6U CompactPCI form factor PC is used as the host computer. The system uses an 850 MHz Pentium III CPU with up to 1 Gigabyte of DRAM.

Rack Assembly

The 19" rack mounted P(Y) HAGR configuration is shown in Figure 8. The chassis houses a standard 6U high CompactPCI backplane. The bottom of the chassis houses cooling fans. The LTG synthesizers are housed in the rear of the chassis.

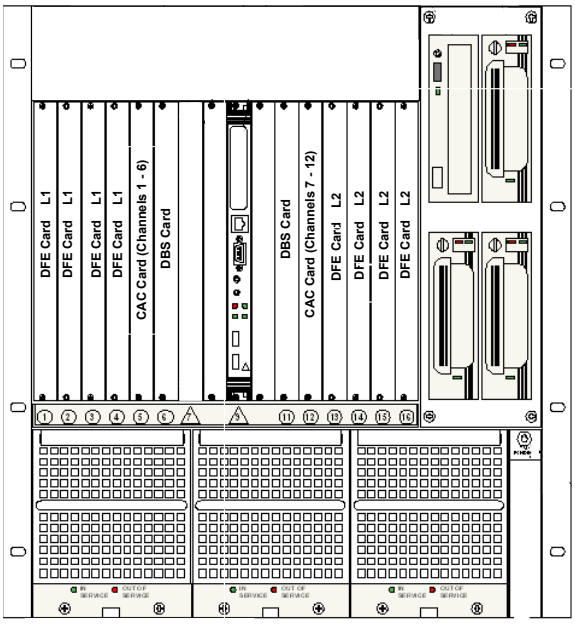

Figure 8 P(Y) HAGR Rack Mount Configuration

DIGITAL BEAM-STEERING OPERATION

The digital beam-steering is performed by applying digital weights to each of the HAGR antenna array outputs using the DBS cards. The weights are applied optimized for each satellite channel, as shown in Figure 2. The digital signal from each of the HAGR antenna elements can be described by the following equation.

Equation 1

$$y_k(t) = \sum_{i=1}^{Ns} s_i(\underline{x}_k, t) + n_k(t)$$

where $s_i(\underline{x}_k,t)$ is the ith GPS satellite signal received at the kth antenna element and $n_k(t)$ is the noise introduced by the kth DFE at the kth antenna element

The GPS satellite signal at each antenna element ($\underline{x}_k$) can be calculated from the following equation.

Equation 2

$$s_i(\underline{x}_k, t) = s_i(0,t)\exp\{-i\frac{2\pi}{\lambda}\underline{1}_i^T\,\underline{x}_k) = s_i(0,t)e_{sik}$$

where $s_i(0,t)$ is the satellite signal at the array center and

$\underline{1}_i$ is the line-of-sight to that satellite

e_{sik} are the elements of a vector of phase angle offsets for satellite i to each element k

The combined digital array signal, z(t), is generated from summing the weighted individual filtered DFE signals. This can be expressed as the following equation.

Equation 3

$$z(t) = \underline{w}'\,\underline{y}(t) = \underline{w}'\left[\sum_{i=1}^{Ns} s_i(t)\underline{e}_{si} + \underline{n}(t)\right]$$

With beam-steering, the optimal weights are selected to maximize the signal/noise ratio to the particular satellite being tracked. These are computed from the satellite phase angle offsets as shown in the following equation.

Equation 4

$$\underline{w}_{BS} = \begin{bmatrix} \exp\{-i\frac{2\pi}{\lambda}\underline{1}_i^T\,\underline{x}_1)\\ \vdots \\ \exp\{-i\frac{2\pi}{\lambda}\underline{1}_i^T\,\underline{x}_M)\end{bmatrix} = \underline{e}_s$$

In Figure 9 and Figure 10, typical L1 and L2 antenna patterns are shown for four satellites in view using the 16-element beam-forming antenna array. As the satellite move across the sky, the beams follow the satellites dynamically adjusting the gain on each of the channels to optimize the signal/noise ratio based on that satellite direction.

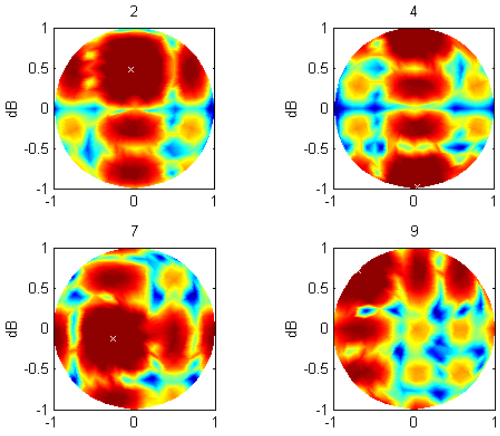

Figure 9 L1 Beam-Steering Pattern

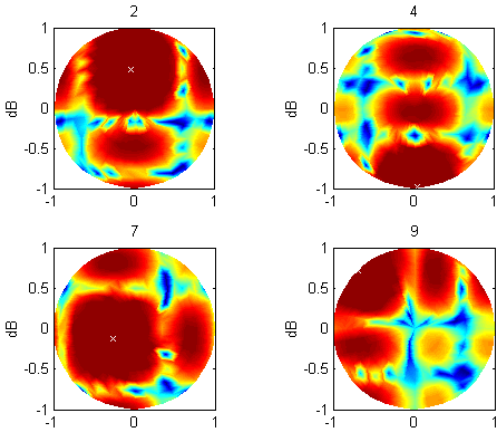

Figure 10 L2 Beam-Steering Pattern

CARRIER PHASE TIME TRANSFER PERFORMANCE

The GPS L1 and L2 pseudo-range and carrier-phase observations are described by the following equations.

Equation 5

$$PR_{i1}(m) = R_i + b_u + \delta b_{u1} - b_{i1} + I_i + \Delta_{Ti} + \tau_{M1i} + n_{PR1}$$

$$PR_{i2}(m) = R_i + b_u + \delta b_{u2} - b_{i1} - \delta b_{i2} + I_i\frac{f_1^2}{f_2^2} + \Delta_{Ti} + \tau_{M2i} + n_{PR2}$$

$$CPH_{i1}(m) = N_1\lambda_1 + n_{CPH1} - (R_i + b_u + \delta b_{c1} - b_{i1} - \delta b_{ic1} - I_i + \Delta_{Ti} + \lambda_1\theta_{M1i})$$

$$CPH_{i2}(m) = N_2\lambda_2 + n_{CPH2} - (R_i + b_u + \delta b_{c2} - b_{i1} - \delta b_{ic2} - I_i\frac{f_1^2}{f_2^2} + \Delta_{Ti} + \lambda_2\theta_{M2i})$$

The following errors affect the pseudo-range and carrier phase observations.

1. Ionosphere errors– these are different on the L1 and L2 PR and CPH observations (I and $I\, f_1^2 / f_2^2$)
2. Troposphere errors – these are the same on all of the observations (Δ_{Ti})
3. Receiver Measurement Noise – these are different on each of the observations (n_{PR1} , n_{PR2} , n_{CPH1} , n_{CPH2})
4. Multipath Noise – these are different on each of the observations (τ_{M1i} , τ_{M2i} , $\lambda_1\theta_{M1i}$, $\lambda_2\theta_{M2i}$)
5. Satellite and Station Position error - these affect the ability to correct for the Range to the satellite (R_i)
6. Station clock and phase offsets on the L1 and L2 signals – these will cancel in the time transfer application (b_{i1} , δb_{i2} , δb_{ic1} , δb_{ic2})
7. Receiver clock calibration errors between the reference clock offset (bu) and the L1 and L2 PR and CPH observations (δb_{u1} , δb_{u2} , δb_{c1} , δb_{c2})

Test results are described in the following sections that characterize the clock calibration stability, and the receiver measurement and multipath noise from the P(Y) HAGR digital beam-steering GPS receiver.

CARRIER PHASE OBSERVATION ACCURACY AND PHASE CALIBRATION STABILITY

The accuracy of the carrier phase observations and the clock calibration stability was observed by connecting two receivers to the same GPS antenna and the same external time reference. The carrier phase observations between the receivers were then differenced to observe the receiver's carrier phase measurement error and any changes in the calibration parameters between the two receivers. The results of these tests for the different satellites tracked are shown in Figure 11 and Figure 12 and summarized in Table 1. This testing shows that the carrier phase observations provided by the HAGR can support picosecond time transfer resolution.

Table 1 Summary of Carrier Phase Time Transfer Observations

SVID	1	14	16	18	22	25
Mean offset (cycles)	.022	.020	.022	.026	.022	.020
Mean offset (psec)	14.3	12.4	14.1	16.8	13.7	12.4
Std Dev (psec)	15.1	17.6	16.3	16.4	15.4	9.2

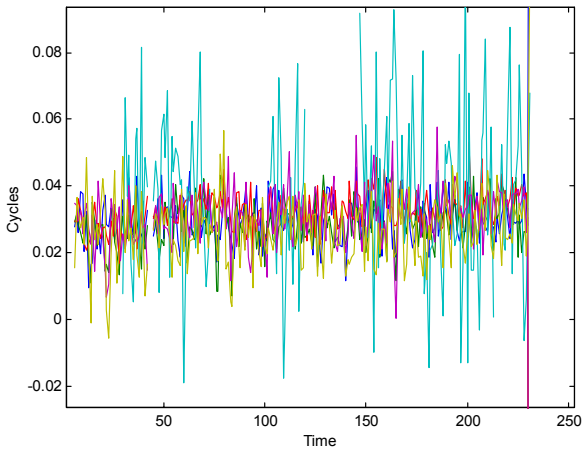

Figure 11 Carrier Phase Difference between Two Units (Test 1) (cycles)

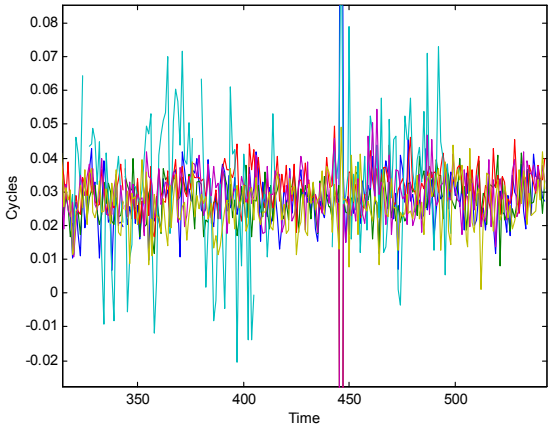

Figure 12 Carrier Phase Difference between Two Units (Test 2) (cycles)

PSEUDO-RANGE MEASUREMENT NOISE AND MULTIPATH ERRORS

The accuracy of the HAGR pseudo-range observations is a function of the received signal strength. A data set was collected to observe the signal-to-noise ratio on the C/A and P(Y) code HAGR data over a period of 12 hours. From this data (Figure 17 and Figure 18) it can be seen that the beam-steering increases the GPS signal strength to a value of 56 dB-Hz on the C/A code. As expected the P(Y) code observed signal strength is 3 dB lower. The predicted pseudo-range noise expected at these signal strength levels is shown in Figure 15. The test data was analyzed to observe the pseudo-range noise and compare it against these predicted accuracies.

From Equation 5, the L1 pseudo-range + carrier phase sum cancels out the common errors and the range to the satellite and observes the pseudo-range and multipath errors as well as the change in the ionospheric offset.

$$
\begin{aligned}
PR_{i1} + CPH_{i1}(m) &= \delta b_{u1} + 2I_i + \tau_{M1i} + n_{PR1} + N_1\lambda_1 + n_{CPH1} \\
&\quad -(\delta b_{c1} - \delta b_{ic1} + \lambda_1\theta_{M1i}) \\
&= C + 2I_i + \tau_{M1i} + n_{PR1} + (n_{CPH1} - \lambda_1\theta_{M1i}) \\
&\approx C + 2I_i + \tau_{M1i} + n_{PR1}
\end{aligned}
$$

The PR+CPH is plotted in Figure 16 for each of the receiver data sets. The short term (<100 sec) white receiver noise was removed by passing the PR+CPH observation through a linear filter. The drift caused by the ionosphere on each observation was removed using a polynomial estimator. The remaining cyclic error is an estimate of the multipath pseudo-range errors. The peak-to-peak cyclic PR variation for each of the receiver data sets was calculated used to estimate the errors observed for each satellite from the pseudo-range multipath[8]. These errors are listed in Table 2 for each of the receiver data sets.

The RMS white noise on the pseudo-range observations was computed by differencing the PR+CPH measurement. This is shown in Figure 17 and Figure 18 for all of the satellites tracked for the C/A and P(Y) code observations. The observed PR noise shows good correspondence with the predicted values shown in Figure 15. For C/N0 values above 52 dB-Hz, the P(Y) code HAGR provided pseudo-range accuracies of 5 cm (1-sigma) while for C/N0 values above 55 dB-Hz the C/A code observations were accurate to 15 cm. These values are for 1-Hz observations without any carrier smoothing applied. The mean observed RMS accuracies are summarized below in Table 2 with the average peak multipath PR errors observed.

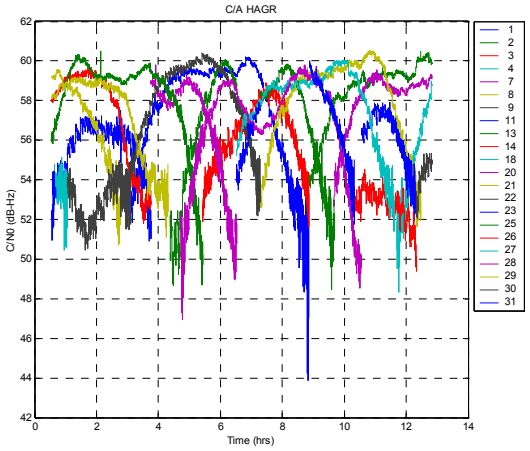

Figure 13 C/A HAGR Signal-to-Noise (dB-Hz)

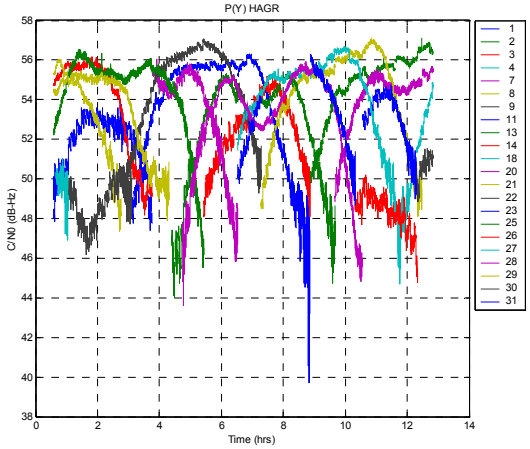

Figure 14 P(Y) HAGR Signal-to-Noise (dB-Hz)

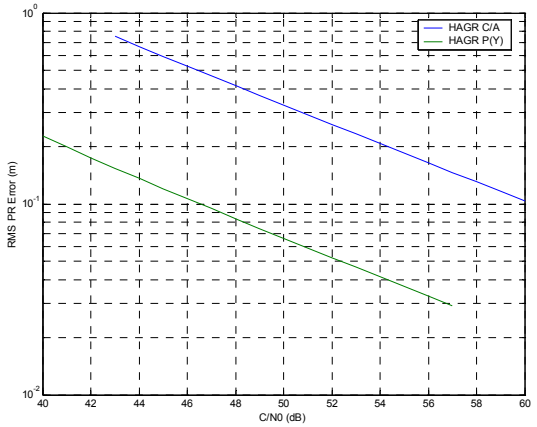

Figure 15 C/A and P(Y) HAGR RMS PR error versus C/N0

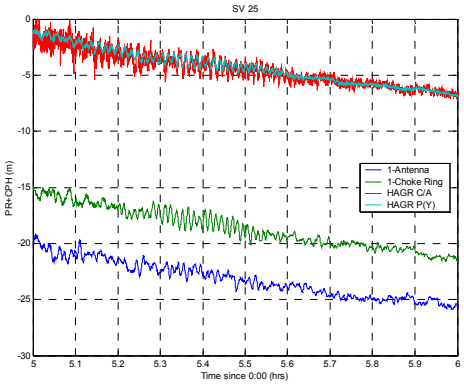

Figure 16 PR+CPH (m) - SV 25

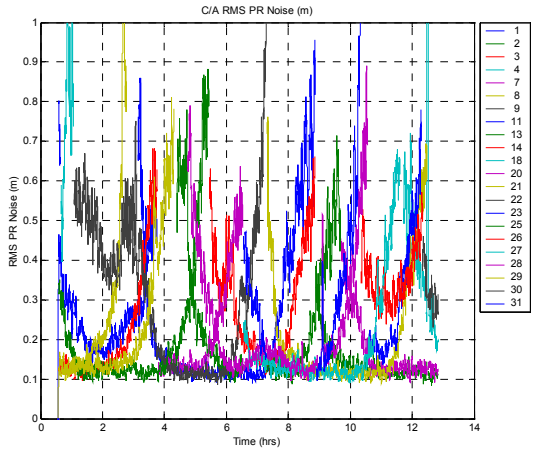

Figure 17 HAGR C/A Code Pseudo-Range Noise (m) (1-Hz DLL – no carrier smothing)

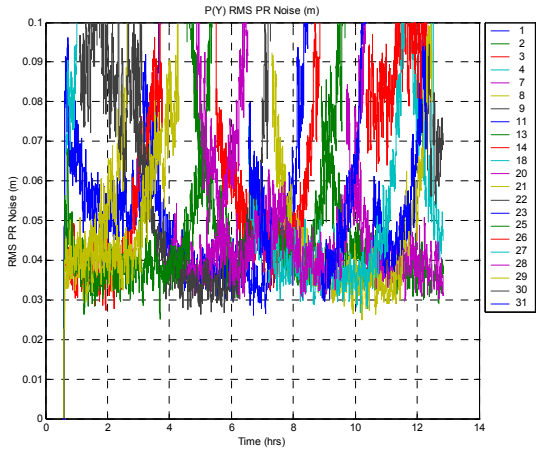

Figure 18 HAGR P(Y) Code Pseudo-Range Noise (m) (1-Hz DLL – no carrier smothing)

Table 2 Mean PR Noise and M-path Peak Errors (m)

SVID	C/A HAGR RMS PR	C/A Mean Mpath PR	P(Y) HAGR RMS PR	P(Y) Mean Mpath PR
1	0.239	0.259	0.054	0.202
3	0.284	0.494	0.056	0.337
8	0.200	0.278	0.045	0.202
11	0.278	0.535	0.059	0.287
13	0.252	0.321	0.059	0.260
14	0.214	0.359	0.049	0.350
20	0.222	0.267	0.050	0.164
21	0.252	0.261	0.058	0.133
22	0.248	0.318	0.047	0.217
25	0.202	0.362	0.044	0.265
27	0.183	0.270	0.044	0.178
28	0.236	0.366	0.055	0.272
29	0.225	0.312	0.050	0.217
30	0.477	0.791	0.089	0.624
31	0.325	0.266	0.055	0.135

CONCLUSION

The testing performed to date on the P(Y) HAGR digital beam-steering GPS receiver has demonstrated the following capabilities.

- Measure the GPS carrier phase noise to an accuracy of 6 mm 1-sigma (20 pico-seconds).
- Measure the GPS P(Y) pseudo-range observations to an accuracy of 5 cm 1-sigma (166 pico-seconds) when the signal/noise ratio is above 52 dB-Hz (includes +10 dB gain from beam-steering)
- Reduce the effect of code multipath through directional beam-steering, which will improve the ability to perform carrier cycle ambiguity resolution

The combination of these capabilities is expected to improve the robustness and precision of GPS carrier time transfer by improving the GPS measurement quality and the ability to perform carrier cycle ambiguity resolution. The HAGR is also designed to provide precise time and phase synchronization to an external time reference.

ACKNOWLEDGMENTS

The P(Y) HAGR is being developed and tested under a contract to the US Naval Observatory.

REFERENCES

[1] K. Larson and J. Levine, "Carrier-Phase Time Transfer" IEEE Transactions on Ultrasonics, Ferroelectronics, and Frequency Control, VOL. 46, NO. 4, July 1999

[2] G. Petit and C. Thomas "GPS Frequency Transfer using Carrier Phase Measurements", Proceedings of the 1996 IEEE Internal Frequency Control Symposium

[3] D. Jefferson, S. Lichten, and L. Young, "A Test of Precision GPS Clock Synchronization" in Proc. 1996 IEEE Freq. Control Symposium, Honolulu, HI, pp. 1206– 1210

[4] T. Schildknecht and T, Springer, "High Precision Time and Frequency Transfer using GPS Phase Measurements", Proceedings of Precise Time and Time Interval (PTTI) Conference, Reston, VA, December 1998

[5] G. Dudle, F. Overney, L. Prost, TH. Schildknecht, T. Springer, P. Hetzel and E. Powers, "First Results on a Transatlantic Time and Frequency Transfer by GPS Carrier Phase", Proceedings of Precise Time and Time Interval (PTTI) Conference, Reston, VA, December 1998

[6] L. Nelson, K. Larson and J. Levine, "Review of GPS Carrier-Phase and Two-Way Satellite Time Transfer

Measurement Results between Schriever Air Force Base and the United States Naval Observatory", Proceedings of ION GPS-99, Nashville, TN, September 1999

[7] N. Gerein, A. Brown, "Modular GPS Software Radio," Proceedings of ION GPS 2001, Salt Lake City, UT, September 2001

[8] A. Brown, N. Gerein, "Test Results from a Digital P(Y) Code Beamsteering Receiver for Multipath Minimization", Proceedings of ION 57th Annual Meeting, Albuquerque, NM, June 2001